Advances in Nano Research, *Vol. 15, No. 1 (2023) 49-57*
https://doi.org/10.12989/anr.2023.15.1.049

Analysis on the influence of sports equipment of fiber reinforced composite material on social sports development

Jian Li[1], Ningjiang Bin[2], Fuqiang Guo[3], Xiang Gao*[4], Renguo Chen[5], Hongbin Yao[6] and Chengkun Zhou[7]

[1]*Asset Management Office, Guangzhou Sport University, Guangzhou 510500, Guangdong, China*
[2]*College of Physical Education, Guangdong University of Education, Guangzhou 510500, Guangdong, China*
[3]*College of Physical Education, Yichun University, Yichun 336000, Jiangxi, China*
[4]*Sport Training Institute, Guangzhou Sport University, Guangzhou 510500, Guangdong, China*
[5]*Physical Education Section, Dongguan NO.10 Senior High School, Dongguan 523981, Guangdong, China*
[6]*School of Humanities and Social Science, Shunde Polytechnic, Foshan 528333, Guangdong, China*
[7]*Graduate school, Guangzhou Sport University, Guangzhou 510500, Guangdong, China*

(*Received April 6, 2022, Revised October 20, 2022, Accepted October 25, 2022*)

Abstract. As composite materials are used in many applications, the modern world looks forward to significant progress. An overview of the application of composite fiber materials in sports equipment is provided in this article, focusing primarily on the advantages of these materials when applied to sports equipment, as well as an Analysis of the influence of sports equipment of fiber-reinforced composite material on social sports development. The present study investigated surface morphology and physical and mechanical properties of S-glass fiber epoxy composites containing Al_2O_3 nanofillers (for example, 1 wt%, 2 wt%, 3 wt%, 4 wt%). A mechanical stirrer and ultrasonication combined the Al_2O_3 nanofiller with the matrix in varying amounts. A compression molding method was used to produce sheet composites. A first physical observation is well done, which confirms that nanoparticles are deposited on the fiber, and adhesive bonds are formed. Al_2O_3 nanofiller crystalline structure was investigated by X-ray diffraction, and its surface morphology was examined by scanning electron microscope (SEM). In the experimental test, nanofiller content was added at a rate of 1, 2, and 3% by weight, which caused a gradual decrease in void fraction by 2.851, 2.533, and 1.724%, respectively, an increase from 2.7%. The atomic bonding mechanism shows molecular bonding between nanoparticles and fibers. At temperatures between 60 °C and 380 °C, Thermogravimetric Analysis (TGA) analysis shows that NPs deposition improves the thermal properties of the fibers and causes negligible weight reduction (percentage). Thermal stability of the composites was therefore presented up to 380 °C. The Fourier Transform Infrared Spectrometer (FTIR) spectrum confirms that nanoparticles have been deposited successfully on the fiber.
Keywords: Al_2O_3; nanofiller; s-glass fiber; social sports; void fraction

1. Introduction

Researchers worldwide are developing new composite materials and experimenting with their applications (Wang *et al*. 2022a). Additionally, these materials have been improved in a variety of ways. As a result of economic development, people's living standards improve, and more people are relaxing in sports venues of all kinds (Rybiński *et al*. 2019). Sports experts are also keen to improve and develop sports equipment as part of the development of modern athletic sports in conjunction with scientific training (Rodríguez-Tobías *et al*. 2019). The lightweight, high strength, and forming characteristics of fiber-reinforced composite materials led to the wide use of these materials in sports equipment (Azman *et al*. 2021). In sports equipment, fiber-reinforced composite materials have many advantages (Lu *et al*. 2011). Before fiber-reinforced composites, wood, steel, stainless steel, and aluminum alloy were the most commonly used materials in sports equipment (Feng and Wang 2022). A significant part of sports equipment relies on human power to move, so it has to be lightweight and requires equipment like tennis rackets, golf clubs, bicycles, skis, and more (Kachere *et al*. 2022). Composite materials reinforced with fibers have an unmatched advantage in this regard (Singh *et al*. 2018). Carbon fiber reinforced golf clubs achieve 70% to 50% improvement in mechanical properties and weight over metal rods with the take-up molding in the carbon fiber cloth. Sports equipment must have excellent mechanical properties so that it is usable (Wen *et al*. 2019). In sports equipment, fiber-reinforced composite materials are more suitable due to their superior strength, modulus, and elastic modulus (Wang *et al*. 2021). Among the reasons for using composite materials as raw materials for sports equipment is their ability to dampen shocks (Ge *et al*. 2021). Technology developments in composite forming have significantly increased its design degrees of freedom, so any product can always find the related material. In this way, forming methods can be adapted to the player's situation and design, and they are easy to maintain and affordable (Afilipoaei and Teodorescu-Draghicescu 2020). A synthetic fiber, glass fibers, such as S-glass fibers, have many properties, including incombustible and resistant to heat,

*Corresponding author, Ph.D.,
E-mail: 65156@gzsport.edu.cn

ISSN: 2287-237X (Print), 2287-2388 (Online)

deformation, and electricity (Abdalla *et al*. 2018). Fibers made of these materials are generally less brittle, extremely flexible at room temperature, and more economical than fibers made of carbon and aramid (Asim *et al*. 2015). Acids and moisture are not a problem for S-glass fibers since they are lightweight and moisture-resistant (Omidi *et al*. 2013; Mousavi *et al*. 2017). The composite matrix should be reinforced with appropriate reinforcing agents to prevent failures (Zhao *et al*. 2022). Modifying the matrix phase is one method of strengthening the matrix phase and improving the properties of the composite. Matrix modification can be accomplished by reinforcing the second phase, consisting of nanotubes, nanowires, and nano-particles (Blachowicz and Ehrmann 2020). To alter the matrix's mechanical, chemical, and physical properties, reinforcement of the second phase is necessary (Su 2014; Xie *et al*. 2018). The secondary phase alters the matrix's multifunctional properties through the physical interaction between the second phase and the matrix. With nano-level fillers, the surface area is large compared to the volume of the surface, so the amount required to achieve mechanical properties is lower than with conventional fillers (in weight percent). For composites fabrication, nanofiller loading content is a crucial factor (Wang 2013; Song *et al*. 2019). Composite material type, filler size, and resin content all contribute to the specific weight fraction of the nanofiller. Research shows a sharp decline in the mechanical properties of composites as the weight fraction of nanofiller content in the matrix rises beyond a specific weight fraction level (wt%) (Moafi and Mostashari 2014). As a result of irregular clusters forming in the matrix, uneven stresses are distributed. The dispersion of nano-size fillers into resin is difficult to accomplish manually (by hand stirring) (Linhares *et al*. 2019).

As a result of recent advancements, researchers have demonstrated that ultrasonication can be used as a method for dispersing filler uniformly (Aoki *et al*. 2019). Composite properties were determined primarily by factors such as particle aspect ratio, the orientation of the filler, size of the filler, filler content (weight%), and homogeneity of the filler dispersion (Wu *et al*. 2020). Previous studies have been conducted on composites' physical, mechanical, and tribological properties containing titanium oxide, nano-silica, nano-alumina, and zirconia as reinforcement materials (Mascia *et al*. 2019). The matrix was reinforced with Al_2O_3 (20-40 nm) because of its excellent properties, such as thermal and chemical stability and multi-functionality. Al_2O_3 plays an essential role in a variety of industrial applications (Ma *et al*. 2020). There have been no preliminary studies on how Al_2O_3 might influence the properties of unidirectional S-glass fiber epoxy composites (Said *et al*. 2020). In this research work, Al_2O_3 will be integrated into the matrix and S-glass fiber using compression molding press techniques, and surface morphology, physical characteristics, and mechanical properties will be examined (Sarkar *et al*. 2019).

2. Experimentation details

In the present composites fabrication, glass fiber is used as the primary reinforcement material. It is a unidirectional S-glass fiber mat (450g/m^3) with a thickness of 0.5 mm and a density of 2.5g/cm^3. Material containing S-glass fibers was sourced from Jushi Pvt. Ltd, India. Materials selected for the fabrication of this kit include LY 556 Epoxy (DIGLYcidyl Ethoxybisphenol A) and HY 951 Hardener (Triethylenetetramine), which have densities of 1.15 and 0.97g/cm^3, respectively (Ning *et al*. 2021; Sheng *et al*. 2021; Luo *et al*. 2023). Huntsman Pvt. provided the matrix materials. As secondary reinforcement material, Al_2O_3 (nanofiller) with particle size and density of 20-40 nm was selected, and Nano Labs Pvt supplied this Al_2O_3 (nanofiller). Ltd, India.

Table 1 Composites designation and their chemical composition

Composite	Chemical composition
Neat resin	S-glass Fiber mat 50 wt% + Matrix 50 wt%
C1	S-glass Fiber mat 50 wt% + Matrix 49 wt% + Al_2O_3 1 wt%
C2	S-glass Fiber mat 50 wt% + Matrix 48 wt% + Al_2O_3 2 wt%
C3	S-glass Fiber mat 50 wt% + Matrix 47 wt% + Al_2O_3 3 wt%
C4	S-glass Fiber mat 50 wt% + Matrix 46 wt% + Al_2O_3 4 wt%
C5	S-glass Fiber mat 50 wt% + Matrix 45 wt% + Al_2O_3 5 wt%

2.1 Fabrication of laminate composites

In order to obtain five fiber mats of equal dimensions for each composite, a continuous S-glass fiber mat was first cut into dimensions of 200 mm x 200 mm (length x width). The manufacturer specified a 10:1 weight ratio for epoxy and hardener in stoichiometry. Table 1 shows the designation of composites and their chemical composition.

Further, S-glass fiber mats, matrixes, and nanofillers were weighted (wt%), 66 ˚C epoxies were heated for 1 hour to lower the liquid's viscosity, then regasified for 20 min at 66 ˚C in a vacuum oven. By using an electronic weighing machine, varying wt% of Al_2O_3 nanofiller were measured (Hou *et al*. 2021; Huang *et al*. 2021b; Xu *et al*. 2021; Wang *et al*. 2022b). By stirring the epoxy at 500 rpm for 30 minutes with weighed Al_2O_3, followed by ultrasonication at 20 kHz for 20 minutes, the weighed Al_2O_3 content was mixed into the epoxy. Increasing Al_2O_3 content increased the ultrasonication process time for better uniform dispersion. By manually stirring with a wood stick, hardener quantity (weight%) was added slowly and steadily to epoxy and mixed for 2 minutes. Layers of glass fiber are then coated with this mixture of liquid matrix and Al_2O_3 at varying weight percentages (Liu *et al*. 2020a, Wang *et al*. 2020, Zhou *et al*. 2020, Dai *et al*. 2021, Guo *et al*. 2021, Shao *et al*. 2021, Wu and Habibi 2021). Composite laminates are fabricated using a compression molding press. An application of a liquid matrix with a roller brush was used in this technique to cover one side of the fiber surface mat uniformly. Over the first layer of the liquid matrix surface mat, a roller brush was used to compress the second layer of fiber mat to remove the excess matrix. This

technique was repeated for five layers with 0 orientation along fiber directions for each composite. After being stacked tightly with all the fiber layers, the composite was placed on the mold die and compressed for 15 minutes at a uniform 5 MPa pressure and temperature of 100 °C, as schematically (Liu *et al*. 2020b, Habibi *et al*. 2021, He *et al*. 2021, Huang *et al*. 2021a, Liu *et al*. 2021, Zhang *et al*. 2021). Varying weight percentages of Al_2O_3 laminate composites with uniform thickness were then cured at room temperature for 48 hours. Still, aromatic amines (hardener compounds) react less with epoxy at room temperature than epoxy. In order to prevent alignment and slope of cross-linked chains that make up matrix, composites are placed in an adjustable mold with holes while curing. Post-cure was done at 80 °C for four hours to strengthen cross-link chain structures. As a final step, composites were characterized and tested by ASTM standards (Ghadiri *et al*. 2017a, b, Mirjavadi *et al*. 2017b, c, Shafiei *et al*. 2017a, b).

3. Characterization techniques of laminate composites

3.1 X-ray diffraction analysis (XRD)

With the help of Ringaku MiniFlex 600, Al_2O_3 nanofiller was characterized. This X-ray source used a voltage of 40 kV and a current of 20 mA. The scanning mode was 2θ, and the scanning speed was 2˚/min. Debye-Scherrer equation (Eq.(1)) was used to calculate the mean crystallite size of the Al_2O_3 nanofiller:

$$D = k\,\lambda / \beta \cos\theta \tag{1}$$

where '*k*' is the dimensionless shape factor (*k*=0.94 for FWHM of spherical crystals with cubic symmetry), 'θ' is the Bragg's diffraction angle, '*D*' is the mean crystallites size (nm), 'λ' is the X-ray source wavelength of 1.54 Å, and 'β' is the Full Width at Half Maximum (FWHM) (Ehyaei *et al*. 2017, Ghadiri *et al*. 2017c, d, Mirjavadi *et al*. 2017d, Shafiei and Kazemi 2017b, Shafiei *et al*. 2017c).

3.2 Scanning electron microscope (SEM)

A laminate composite with variable Al_2O_3 concentration on the resin surface was cut into 10 mm x 10 mm (length x width) dimensions for surface morphology study. A scanning electron microscope (ZEISS EVO 18) was then used to examine the prepared specimens. Carbon tape was used to mount specimens on the aluminum multi-pin stubs. With a 15.00 kV accelerating voltage, the instrument was operated (Ebrahimi and Shafiei 2017, Ghadiri *et al*. 2017e, Mirjavadi *et al*. 2017a, Shafiei and Kazemi 2017a, Shafiei *et al*. 2017d, Azimi *et al*. 2018).

3.3 Density and void fraction

The fraction of voids in polymer composites is an important characteristic that determines the quality of the composite and its span (Shafiei and She 2018, Shafiei *et al*. 2019, 2020).

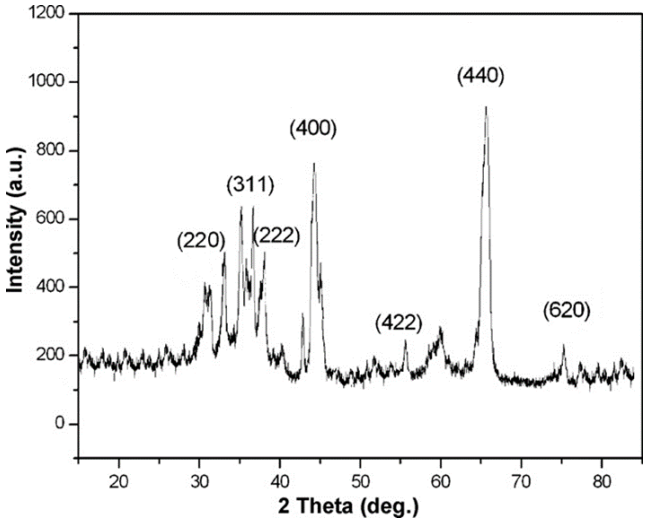

Fig. 1 Different scanning angles of Al_2O_3 nanofiller's X-ray diffraction peaks

3.4 Thermal characterization

A thermogravimetric analysis (TGA) was conducted on fabricated composites to determine their thermal stability. According to ASTM E1131, the PERKIN ELMER TGA 4000 is in a closed atmosphere chamber with nitrogen gas flowing at 60 ml per minute and a specimen weight of 10 mg. Different controlled temperature ranges were applied to specimens in this test method. Heating samples achieved a temperature range of 60 to 900°C at 20 °C per minute. As a function of temperature variations in a closed, controlled environment, the weight loss (%) is measured in the composites (Ebrahimi and Shafiei 2016, Shafiei *et al*. 2016a, b, c, Ebrahimi *et al*. 2017, Shivanian *et al*. 2017).

4. Results and discussions

4.1 X-ray diffraction analysis of Al2O3 nanofiller

4.1.1 Al_2O_3 peak indexing

It was determined that the Al_2O_3 nanofiller has a crystalline structure by using X-ray diffraction. An XRD pattern of nanofiller diffraction peaks is shown in Fig. 1 at various scanning angles. Based on Fig. 1, it can be seen that the characteristic diffraction peaks obtained from the Al_2O_3 nanofiller are consistent with those observed for hexagonal wurtzite structures containing the Al_2O_3 space group. XRD patterns revealed sharp, narrow, broad varying diffraction peaks that were associated with Al_2O_3's good crystalline nature (Li *et al*. 2022, Tang *et al*. 2022, Xue *et al*. 2022, Zhang *et al*. 2022, Cao *et al*. 2023, Zhao *et al*. 2023).

This means that there was no sign of remnant micro and foreign particles in Al_2O_3 as purchased. The mean crystallite size of Al_2O_3 at strong peak diffraction was calculated using the Debye-Scherrer equation. According to XRD patterns, a = 7.951 was the lattice parameter. Based on the 400-line width of the XRD peaks of the sample, the particle size was

Table 2 Size, d-spacing, and space lattice plane of the crystallites in Al_2O_3 at firm diffraction peaks

Material	Peak/2θ	FWHM	Space lattice	d-spacing	Mean crystallites
Al_2O_3	31.41	0.364	(220)	2.963	25.12
	35.89	0.293	(311)	2.630	29.89
	38.32	0.372	(222)	2.561	24.84
	45.63	0.350	(400)	1.968	27.69
	56.21	0.384	(422)	1.795	25.38
	63.27	0.345	(440)	1.526	28.74
	78.11	0.371	(620)	1.482	26.58

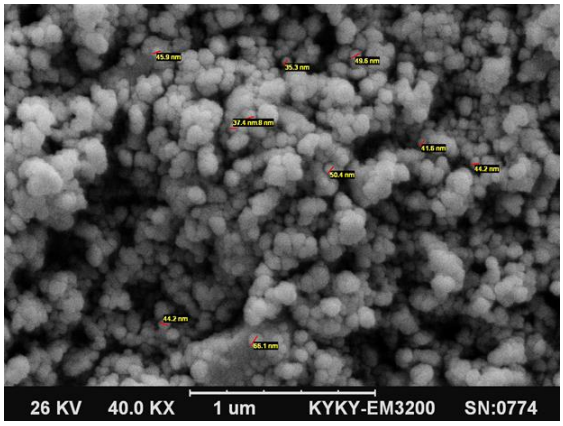

Fig. 2 Nanofiller Al_2O_3 dispersion on resin surface

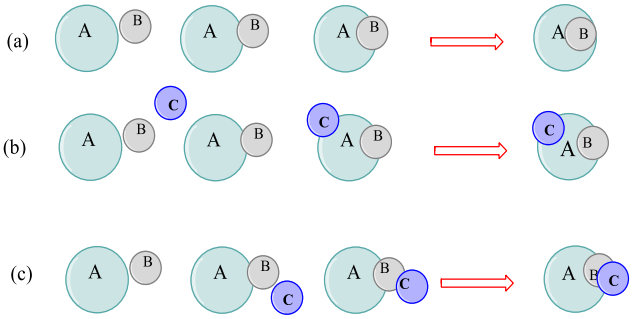

Fig. 3 Different mechanisms of cluster formation with ultrasonication in resin

determined to be 10 nanometers. Al_2O_3 peaks with strong diffraction peaks are shown in Table 2, along with their mean crystallite size, d-spacing, and lattice planes.

4.2 Surface morphology of Al2O3 nanofiller on the resin surface

ZEISS EVO 18 scanning electron microscopes were used to examine the surface morphology of Al_2O_3 nanofiller on resin surfaces. Al_2O_3 nanofiller disperses on resin surface according to its dispersion state, as shown in Fig. 2. Based on the SEM images of resin surfaces that contain 1 wt% and 2 wt% of Al_2O_3 nanofiller, it is evident that they have almost homogenous, uniform dispersion and spheroid-shaped structures. Optimal ultrasonication techniques and low nanofiller loading content (weight%) both contributed to uniform dispersion on the resin surface. Nanofiller occupies a sparse amount of surface area in resin at such a low loading, thus, van der Waals forces (physical forces) between the nanofiller are negligible, allowing uniform dispersion and thereby maintaining the uniform shape. As a result of interaction between nanofillers, a variety of shapes and sizes were observed. Nanofiller diameters were also slightly increased to micron level as a result of colliding. Al_2O_3 nanofiller at 3 wt% in the resin is also perceived as improving dispersion and reducing the possibility of voids, thus improving interfacial bond strength between fiber laminates. Because of the low surface-to-volume ratio of resins, the nanofiller occupies short inter-particle distances after loading Al_2O_3 to 4 wt%, where they agglomerate and overlap because of van der Waals interactions. With loading to 5 wt%, inter-particle distances become smaller than those when laden to 4 wt%, which results in large uneven clusters colliding and forming voids at the collided interfaces.

4.2.1 Effect of Al_2O_3 morphology by cluster growth mechanism

Nanoparticles display their properties in cluster growth mechanisms based on their structure, which results in particle growth. As a result of the SEM study, cluster generation was found to influence Al_2O_3 (wt%), stirring process, and stirring time significantly. In the SEM images with a variable weight percentage of Al_2O_3, the low weight percentage had negligible clusters, meaning that particles did not interact (van der Waals forces) with each other in the epoxy volume. By reducing the particle volume/epoxy volume ratio, more and more clusters are being formed as the weight percentage increases because individual nanoparticles start colliding with one another, resulting in cluster formation. Due to their larger surface volume, clusters created by self-assembling nanoparticles have greater interaction with one another, attracting more nanoparticles and clusters within the same space. During ultrasonication, clusters may collide in a reduced volume ratio area, leading to agglomeration or coalescence that is larger than the clusters that originated. The clustering mechanism in this work can be explained through the diffusion process of nanoparticles, as shown in Fig. 3. During the first mechanism (a), the surface of particle B attracts cluster A through gravity or van der Waals forces, gradually enmeshing the particle in the cluster. However, in mechanism (b), particles like B and C collide with the cluster surface one by one and slowly merge into the cluster to form a larger cluster. Fig. 3 illustrates how mechanism (c) proposes that first individual particles B will attract the surface of the cluster, then particle C will collide with the surface of particle B, and they will eventually all merge together, forming a large and uneven cluster. According to data, coagulation of the particles has a great influence on time, as gravity and diffusion help the particles settle down after ultrasonication. By using different cluster mechanisms, particles will collide with each other in this process. As a result, the time between sonication and afterward is crucial to cluster formation.

4.3 Thermo-gravimetric test results and analysis (TGA)

The thermogravimetric analysis aimed to determine composites' thermal stability and performance at elevated

Table 3 Characteristic of weight loss (%) in composites with the function of temperature

Composite	Al_2O_3 (wt%)	Onset(°C)	First characteristic weight loss (%) 380˚C - 600˚C	Second characteristic weight loss (%) 600˚C - 900˚C
Neat resin	0	380.50	48.325	7.887
C1	1	380.59	46.538	7.465
C2	2	380.79	42.209	6.986
C3	3	381.10	37.520	5.358
C4	4	381.21	38.853	5.833
C5	5	380.97	39.971	6.857

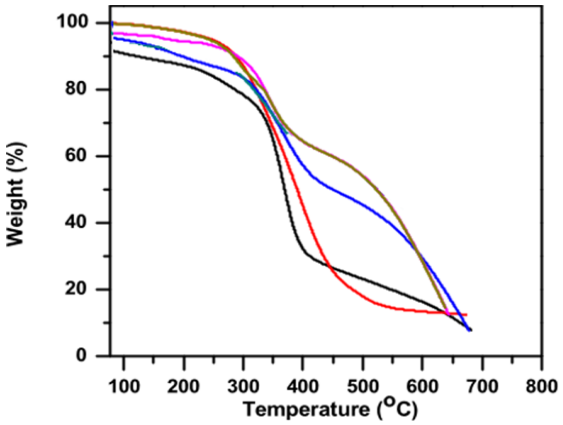

Fig. 4 Stages of weight loss (%) in composites with the function of temperature

temperatures. As illustrated in Fig. 4, it describes how weight loss (%) varies with temperature variations in composites. Table 3 lists the composites' weight loss (%) as a function of temperature variations.

In composites, the slight weight loss (2-3%) occurs due to the loss of bound moisture content and volatilization (unreacted epoxy/hardener compounds, bound gases, monomers.) from the matrix during the dehydration process at temperatures ranging from 50 to 380 °C. Almost no weight loss (%) was observed for almost every composite up to 380 °C. Weight loss (%) in composites occurs at a range of temperatures between 380 and 600 °C. This temperature range causes increased heat radiation to cause the matrix inside the layers to depolymerize and plasticize. Because of the plasticization effect, nanofiller content gradually decreases its adhesive nature with the matrix as the composite microstructure changes (matrix and glass fiber microstructures). At temperatures between 380 °C and 600 °C, this causes a breakdown of the polymer backbone cross-link chain structure between epoxy, hardener, and nanofiller, characterizing a breakdown of the polymer backbone cross-link chain structure. Initiation degradation point refers to the moment when composites begin to degrade.

A neat resin composite containing no filler exhibits a tremendous weight loss at 48.157% from the first degradation stage. In contrast, composites with varying Al_2O_3 nanofiller content showed weight losses of 46.538, 42.209, 37.520, 38.853, and 39.971%, corresponding to 1, 2, 3, 4, and 5 wt% nanofiller content. In composites, the characteristic trends in weight loss (%) were primarily due to Al_2O_3 nanofiller inclusion. By providing rigid cross-linking chain structures, nanofiller content in the matrix can create more resistance to heat radiation. During the first degradation stage, weight loss (%) decreases slightly with filler content but increases by 38.853 and 39.971% for 3 and 4 weight percent of reinforcement. Composites with 4 to 5 wt% reinforcement may experience increased weight loss (%) because the polymer chains (OH groups) are weakened and broken, as Al_2O_3 clusters act as barriers to the polymer chain mobility structure and break down epoxy-OH bonding groups at those wt% reinforcements.

5. Conclusions

In this study, Al_2O_3 nanofiller was added to S-glass fiber epoxy composites to study the influence of matrix modification. A variety of properties of composites were evaluated, including surface morphology, mechanical properties, and physical properties. An SEM analysis of the surface morphology of Al_2O_3 nanofiller on resin surface showed that at 1, 2, and 3 wt% loadings, a more uniform dispersion was achieved through ultrasonication. As loading increased from 4 and 5 wt% to 5 wt%, uneven clusters were formed on the resin surface due to increased loading levels, which increased van der Waals interaction forces among nanofiller. Based on thermogravimetric analysis of composites, they were thermally stable in the range of 60 °C to 380 °C with minimal weight loss (%). In addition, there was significant thermal degradation at temperatures over 380°C (to 900°C), indicated by significant weight loss (%) as the temperature increased. Composites with decreased weight losses (%) were attributed to volatilization, matrix plasticization, and depolymerization effects. According to the study, these composites could be used at temperatures below 380 °C. Based on surface morphology, void fraction, and flexure and impact results, it was observed that composites with 3 wt% of Al_2O_3 nanofiller loading had the best nanofiller dispersion, strength (flexure/impact), and void content. The S-glass fiber-reinforced composite with 3 wt% Al_2O_3 can be used in aircraft, sports equipment, and boat hulls when high mechanical loads are applied to the target areas.

References

Abdalla, I., Shen, J., Yu, J., Li, Z. and Ding, B. (2018), "Co3O4/carbon composite nanofibrous membrane enabled high-efficiency electromagnetic wave absorption", *Sci. Rep.*, **8**(1), 12402. https://doi.org/10.1038/s41598-018-30871-2.

Afilipoaei, C. and Teodorescu-Draghicescu, H. (2020), "A review

over electromagnetic shielding effectiveness of composite materials", *Proceedings*, **63**(1), 23. https://doi.org/10.3390/proceedings2020063023.

Al-Furjan, M., Moghadam, S.A., Dehini, R., Shan, L., Habibi, M. and Safarpour, H. (2020), "Vibration control of a smart shell reinforced by graphene nanoplatelets under external load: Semi-numerical and finite element modeling", *Thin Wall. Struct.*, 107242. https://doi.org/10.1016/j.tws.2020.107242.

Aoki, R., Yamaguchi, A., Hashimoto, T., Urushisaki, M., Sakaguchi, T., Kawabe, K., Kondo, K. and Iyo, H. (2019), "Preparation of carbon fibers coated with epoxy sizing agents containing degradable acetal linkages and synthesis of carbon fiber-reinforced plastics (CFRPs) for chemical recycling", *Polym. J.*, **51**(9), 909-920. https://doi.org/10.1038/s41428-019-0202-7.

Asim, M., Abdan, K., Jawaid, M., Nasir, M., Dashtizadeh, Z., Ishak, M.R. and Hoque, M.E. (2015), "A review on pineapple leaves fibre and its composites", *Int. J. Polym. Sci.*, **2015**, 950567. https://doi.org/10.1155/2015/950567.

Azimi, M., Mirjavadi, S.S., Shafiei, N., Hamouda, A.M.S. and Davari, E. (2018), "Vibration of rotating functionally graded Timoshenko nano-beams with nonlinear thermal distribution", *Mech. Adv. Mater. Struct.*, **25**(6), 467-480. https://doi.org/10.1080/15376494.2017.1285455.

Azman, M.A., Asyraf, M.R.M., Khalina, A., Petrů, M., Ruzaidi, C.M., Sapuan, S.M., Wan Nik, W.B., Ishak, M.R., Ilyas, R.A. and Suriani, M.J. (2021), "Natural fiber reinforced composite material for product design: A short review", *Polymers*, **13**(12), 1917. https://doi.org/10.3390/polym13121917.

Blachowicz, T. and Ehrmann, A. (2020), "Recent developments in electrospun ZnO nanofibers: A short review", *J. Eng. Fibers Fabr.*, **15**, 1558925019899682. https://doi.org/10.1177/1558925019899682.

Cao, Z., Niu, B., Zong, G., Zhao, X. and Ahmad, A.M. (2023), "Active disturbance rejection-based event-triggered bipartite consensus control for nonaffine nonlinear multiagent systems", *Int. J. Robust Nonlinear Control.*, **n/a**(n/a). https://doi.org/10.1002/rnc.6746.

Cheshmeh, E., Karbon, M., Eyvazian, A., Jung, D.w., Habibi, M. and Safarpour, M. (2020), "Buckling and vibration analysis of FG-CNTRC plate subjected to thermo-mechanical load based on higher order shear deformation theory", *Mech. Based Des. Struct.*, 1-24. https://doi.org/10.1080/15397734.2020.1744005.

Dai, Z., Jiang, Z., Zhang, L. and Habibi, M. (2021), "Frequency characteristics and sensitivity analysis of a size-dependent laminated nanoshell", *Adv. Nano Res.*, **10**(2), 175. https://doi.org/10.12989/anr.2021.10.2.175.

Ebrahimi, F. and Shafiei, N. (2016), "Application of Eringen's nonlocal elasticity theory for vibration analysis of rotating functionally graded nanobeams", *Smart Struct. Syst.*, **17**(5), 837-857. https://doi.org/10.12989/sss.2016.17.5.837.

Ebrahimi, F. and Shafiei, N. (2017), "Influence of initial shear stress on the vibration behavior of single-layered graphene sheets embedded in an elastic medium based on Reddy's higher-order shear deformation plate theory", *Mech. Adv. Mater. Struct.*, **24**(9), 761-772. https://doi.org/10.1080/15376494.2016.1196781.

Ebrahimi, F., Shafiei, N., Kazemi, M. and Mousavi Abdollahi, S.M. (2017), "Thermo-mechanical vibration analysis of rotating nonlocal nanoplates applying generalized differential quadrature method", *Mech. Adv. Mater. Struct.*, **24**(15), 1257-1273. https://doi.org/10.1080/15376494.2016.1227499.

Ehyaei, J., Akbarshahi, A. and Shafiei, N. (2017), "Influence of porosity and axial preload on vibration behavior of rotating FG nanobeam", *Adv. Nano Res.*, **5**(2), 141. https://doi.org/10.12989/anr.2017.5.2.141.

Feng, Q. and Wang, L. (2022), "The effect of polymer composite materials on the comfort of sports and fitness facilities", *J. Nanomater.*, **2022**, 9108458. https://doi.org/10.1155/2022/9108458.

Ge, L., Yin, J., Yan, D., Hong, W. and Jiao, T. (2021), "Construction of nanocrystalline cellulose-based composite fiber films with excellent porosity performances via an electrospinning strategy", *ACS Omega*, **6**(7), 4958-4967. https://doi.org/10.1021/acsomega.0c06002.

Ghadiri, M., Mahinzare, M., Shafiei, N. and Ghorbani, K. (2017a), "On size-dependent thermal buckling and free vibration of circular FG Microplates in thermal environments", *Microsyst. Technol.*, **23**(10), 4989-5001. https://doi.org/10.1007/s00542-017-3308-x.

Ghadiri, M., Shafiei, N. and Alavi, H. (2017b), "Thermo-mechanical vibration of orthotropic cantilever and propped cantilever nanoplate using generalized differential quadrature method", *Mech. Adv. Mater. Struct.*, **24**(8), 636-646. https://doi.org/10.1080/15376494.2016.1196770.

Ghadiri, M., Shafiei, N. and Alavi, H. (2017c), "Vibration analysis of a rotating nanoplate using nonlocal elasticity theory", *J. Solid Mech.*, **9**(2), 319-337.

Ghadiri, M., Shafiei, N. and Babaei, R. (2017d), "Vibration of a rotary FG plate with consideration of thermal and Coriolis effects", *Steel Compos. Struct.*, **25**(2), 197-207. https://doi.org/10.12989/SCS.2017.25.2.197.

Ghadiri, M., Shafiei, N. and Safarpour, H. (2017e), "Influence of surface effects on vibration behavior of a rotary functionally graded nanobeam based on Eringen's nonlocal elasticity", *Microsyst. Technol.*, **23**(4), 1045-1065. https://doi.org/10.1007/s00542-016-2822-6.

Guo, J., Baharvand, A., Tazeddinova, D., Habibi, M., Safarpour, H., Roco-Videla, A. and Selmi, A. (2021), "An intelligent computer method for vibration responses of the spinning multi-layer symmetric nanosystem using multi-physics modeling", *Eng. Comput.*, 1-22. https://doi.org/10.1007/s00366-021-01433-4.

Habibi, M., Darabi, R., Sa, J.C.d. and Reis, A. (2021), "An innovation in finite element simulation via crystal plasticity assessment of grain morphology effect on sheet metal formability", *Proceedings of the Institution of Mechanical Engineers, Part L: Journal of Materials: Design and Applications*, **235**(8), 1937-1951. https://doi.org/10.1177/14644207211024686.

Hashemi, H.R., Alizadeh, A.a., Oyarhossein, M.A., Shavalipour, A., Makkiabadi, M. and Habibi, M. (2019), "Influence of imperfection on amplitude and resonance frequency of a reinforcement compositionally graded nanostructure", *Waves Random Complex Med.*, 1-27. https://doi.org/10.1080/17455030.2019.1662968.

He, X., Ding, J., Habibi, M., Safarpour, H. and Safarpour, M. (2021), "Non-polynomial framework for bending responses of the multi-scale hybrid laminated nanocomposite reinforced circular/annular plate", *Thin Wall. Struct.*, **166**, 108019. https://doi.org/10.1016/j.tws.2021.108019.

Hou, F., Wu, S., Moradi, Z. and Shafiei, N. (2021), "The computational modeling for the static analysis of axially functionally graded micro-cylindrical imperfect beam applying the computer simulation", *Eng. Comput.*, 1-19. https://doi.org/10.1007/s00366-021-01456-x.

Huang, X., Hao, H., Oslub, K., Habibi, M. and Tounsi, A. (2021a), "Dynamic stability/instability simulation of the rotary size-dependent functionally graded microsystem", *Eng. Comput.*, 1-17. https://doi.org/10.1007/s00366-021-01399-3.

Huang, X., Zhang, Y., Moradi, Z. and Shafiei, N. (2021b), "Computer simulation via a couple of homotopy perturbation methods and the generalized differential quadrature method for nonlinear vibration of functionally graded non-uniform micro-

tube", *Eng*. *Comput*., 1-18. https://doi.org/10.1007/s00366-021-01395-7.

Kachere, A.R., Kakade, P.M., Kanwade, A.R., Dani, P., N, N., M, k.T., lik, l., Rondiya, S.R., Dzade, N.Y., S, S., Jadkar, e.R. and Bhosale, S.V. (2022), "Zinc oxide/graphene oxide nano-composites: Synthesis, characterization and their optical properties", *ES Mater*. *Manuf.*, **16**, 19-29. https://doi.org/10.30919/esmm5f516.

Li, Y., Wang, H., Zhao, X. and Xu, N. (2022), "Event-triggered adaptive tracking control for uncertain fractional-order nonstrict-feedback nonlinear systems via command filtering", *Int. J. Robust Nonlinear Control*, **32**(14), 7987-8011. https://doi.org/10.1002/rnc.6255.

Linhares, T., Pessoa de Amorim, M.T. and Durães, L. (2019), "Silica aerogel composites with embedded fibres: a review on their preparation, properties and applications", *J. Mater. Chem. A*, **7**(40), 22768-22802. https://doi.org/10.1039/C9TA04811A.

Liu, H., Zhao, Y., Pishbin, M., Habibi, M., Bashir, M. and Issakhov, A. (2021), "A comprehensive mathematical simulation of the composite size-dependent rotary 3D microsystem via two-dimensional generalized differential quadrature method", *Eng*. *Comput*., 1-16. https://doi.org/10.1007/s00366-021-01419-2.

Liu, Z., Su, S., Xi, D. and Habibi, M. (2020a), "Vibrational responses of a MHC viscoelastic thick annular plate in thermal environment using GDQ method", *Mech*. *Based Des*. *Struct*., 1-26. https://doi.org/10.1080/15397734.2020.1784201.

Liu, Z., Wu, X., Yu, M. and Habibi, M. (2020b), "Large-amplitude dynamical behavior of multilayer graphene platelets reinforced nanocomposite annular plate under thermo-mechanical loadings", *Mech*. *Based Des*. *Struct*., 1-25. https://doi.org/10.1080/15397734.2020.1815544.

Lori, E.S., Ebrahimi, F., Supeni, E.E.B., Habibi, M. and Safarpour, H. (2020), "The critical voltage of a GPL-reinforced composite microdisk covered with piezoelectric layer", *Eng*. *Comput*., 1-20. https://doi.org/10.1007/s00366-020-01004-z.

Lu, N., Swan, R.H. and Ferguson, I. (2011), "Composition, structure, and mechanical properties of hemp fiber reinforced composite with recycled high-density polyethylene matrix", *J. Compos*. *Mater*., **46**(16), 1915-1924. https://doi.org/10.1177/0021998311427778.

Luo, G., Xie, J., Liu, J., Zhang, Q., Luo, Y., Li, M., Zhou, W., Chen, K., Li, Z., Yang, P., Zhao, L., Siong Teh, K., Wang, X., Dong, L., Maeda, R. and Jiang, Z. (2023), "Highly conductive, stretchable, durable, breathable electrodes based on electrospun polyurethane mats superficially decorated with carbon nanotubes for multifunctional wearable electronics", *Chem*. *Eng*. *J*., **451**, 138549. https://doi.org/10.1016/j.cej.2022.138549.

Ma, K., Idrees, K.B., Son, F.A., Maldonado, R., Wasson, M.C., Zhang, X., Wang, X., Shehayeb, E., Merhi, A., Kaafarani, B.R., Islamoglu, T., Xin, J.H. and Farha, O.K. (2020), "Fiber composites of metal–organic frameworks", *Chem*. *Mater*., **32**(17), 7120-7140. https://doi.org/10.1021/acs.chemmater.0c02379.

Mascia, L., Zhang, W., Gatto, F., Scarpellini, A., Pompa, P.P. and Mele, E. (2019), "In situ generation of ZnO nanoparticles within a polyethyleneimine matrix for antibacterial zein fibers", *ACS Appl*. *Polym*. *Mater*., **1**(7), 1707-1716. https://doi.org/10.1021/acsapm.9b00276.

Mirjavadi, S.S., Afshari, B.M., Shafiei, N., Hamouda, A., Kazemi, M. and Structures, C. (2017a), "Thermal vibration of two-dimensional functionally graded (2D-FG) porous Timoshenko nanobeams", *Steel Compos*. *Struct*., **25**(4), 415-426. https://doi.org/10.12989/scs.2017.25.4.415.

Mirjavadi, S.S., Matin, A., Shafiei, N., Rabby, S. and Mohasel Afshari, B. (2017b), "Thermal buckling behavior of two-dimensional imperfect functionally graded microscale-tapered porous beam", *J. Therm*. *Stress*., **40**(10), 1201-1214. https://doi.org/10.1080/01495739.2017.1332962.

Mirjavadi, S.S., Mohasel Afshari, B., Shafiei, N., Rabby, S. and Kazemi, M. (2017c), "Effect of temperature and porosity on the vibration behavior of two-dimensional functionally graded micro-scale Timoshenko beam", *J. Vib*. *Control*, **24**(18), 4211-4225. https://doi.org/10.1177/1077546317721871.

Mirjavadi, S.S., Rabby, S., Shafiei, N., Afshari, B.M. and Kazemi, M. (2017d), "On size-dependent free vibration and thermal buckling of axially functionally graded nanobeams in thermal environment", *Appl*. *Phys*. *A*, **123**(5), 315. https://doi.org/10.1007/s00339-017-0918-1.

Moafi, H.F. and Mostashari, S.M. (2014), "Flame-resistant polymeric composite fibers based on nanocoating flame retardant: thermogravimetric study and production of α-Al2O3 nanoparticles by flame combustion", *J. Polym. Eng*., **34**(9), 803-812. https://doi.org/10.1515/polyeng-2013-0176.

Mousavi, S.M., Shafiei, N. and Dadvand, A. (2017), "Numerical simulation of subsonic turbulent flow over NACA0012 airfoil: Evaluation of turbulence models", *Sigma J. Eng. Natural Sci*., **35**(1), 133-155. https://dergipark.org.tr/en/pub/sigma/issue/65585/1016455#article_cite.

Najaafi, N., Jamali, M., Habibi, M., Sadeghi, S., Jung, D.w. and Nabipour, N. (2020), "Dynamic instability responses of the substructure living biological cells in the cytoplasm environment using stress-strain size-dependent theory", *J. Biomol. Struct. Dyn*., 1-12. https://doi.org/10.1080/07391102.2020.1751297.

Ning, F., He, G., Sheng, C., He, H., Wang, J., Zhou, R. and Ning, X. (2021), "Yarn on yarn abrasion performance of high modulus polyethylene fiber improved by graphene/polyurethane composites coating", *J. Eng. Fibers Fabr*., **16**, 1558925020983563. https://doi.org/10.1177/1558925020983563.

Omidi, S., Oskooee, M.B. and Shafiei, N. (2013), "Finite element analysis of an ultra-fine grained Titanium dental implant covered by different thicknesses of hydroxyapatite layer", *Indian J. Dent*., **4**(1), 1-4. https://doi.org/10.1016/j.ijd.2012.10.002.

Rodríguez-Tobías, H., Morales, G. and Grande, D. (2019), "Comprehensive review on electrospinning techniques as versatile approaches toward antimicrobial biopolymeric composite fibers", *Mater. Sci. Eng. C*, **101**, 306-322. https://doi.org/10.1016/j.msec.2019.03.099.

Rybiński, P., Syrek, B., Żukowski, W., Bradło, D., Imiela, M., Anyszka, R., Blume, A. and Verbouwe, W. (2019), "Impact of basalt filler on thermal and mechanical properties, as well as fire hazard, of silicone rubber composites, including ceramizable composites", *Materials*, **12**(15), 2432. https://doi.org/10.3390/ma12152432.

Said, S., Mikhail, S. and Riad, M. (2020), "Recent processes for the production of alumina nano-particles", *Mater. Sci. Energy Technol*., **3**, 344-363. https://doi.org/10.1016/j.mset.2020.02.001.

Sarkar, C., Sahu, S.K., Sinha, A., Chakraborty, J. and Garai, S. (2019), "Facile synthesis of carbon fiber reinforced polymer-hydroxyapatite ternary composite: A mechanically strong bioactive bone graft", *Mater. Sci. Eng. C*, **97**, 388-396. https://doi.org/10.1016/j.msec.2018.12.064.

Shafiei, N., Ghadiri, M. and Mahinzare, M. (2019), "Flapwise bending vibration analysis of rotary tapered functionally graded nanobeam in thermal environment", *Mech. Adv. Mater. Struct*., **26**(2), 139-155. https://doi.org/10.1080/15376494.2017.1365982.

Shafiei, N., Ghadiri, M., Makvandi, H. and Hosseini, S.A. (2017a), "Vibration analysis of Nano-Rotor's Blade applying Eringen nonlocal elasticity and generalized differential

quadrature method", *Appl. Math. Modell.*, **43**, 191-206. https://doi.org/10.1016/j.apm.2016.10.061.

Shafiei, N., Hamisi, M. and Ghadiri, M. (2020), "Vibration analysis of rotary tapered axially functionally graded Timoshenko nanobeam in thermal environment", *J. Solid Mech.*, **12**(1), 16-32.

Shafiei, N. and Kazemi, M. (2017a), "Buckling analysis on the bi-dimensional functionally graded porous tapered nano-/micro-scale beams", *Aerosp. Sci. Technol.*, **66**, 1-11. https://doi.org/10.1016/j.ast.2017.02.019.

Shafiei, N. and Kazemi, M. (2017b), "Nonlinear buckling of functionally graded nano-/micro-scaled porous beams", *Compos. Struct.*, **178**, 483-492. https://doi.org/10.1016/j.compstruct.2017.07.045.

Shafiei, N., Kazemi, M. and Fatahi, L. (2017b), "Transverse vibration of rotary tapered microbeam based on modified couple stress theory and generalized differential quadrature element method", *Mech. Adv. Mater. Struct.*, **24**(3), 240-252. https://doi.org/10.1080/15376494.2015.1128025.

Shafiei, N., Kazemi, M. and Ghadiri, M. (2016a), "Nonlinear vibration of axially functionally graded tapered microbeams", *Int. J. Eng. Sci.*, **102**, 12-26. https://doi.org/10.1016/j.ijengsci.2016.02.007.

Shafiei, N., Kazemi, M. and Ghadiri, M. (2016b), "On size-dependent vibration of rotary axially functionally graded microbeam", *Int. J. Eng. Sci.*, **101**, 29-44. https://doi.org/10.1016/j.ijengsci.2015.12.008.

Shafiei, N., Mirjavadi, S.S., Afshari, B.M., Rabby, S. and Hamouda, A.M.S. (2017c), "Nonlinear thermal buckling of axially functionally graded micro and nanobeams", *Compos. Struct.*, **168**, 428-439. https://doi.org/10.1016/j.compstruct.2017.02.048.

Shafiei, N., Mirjavadi, S.S., MohaselAfshari, B., Rabby, S. and Kazemi, M. (2017d), "Vibration of two-dimensional imperfect functionally graded (2D-FG) porous nano-/micro-beams", *Comput. Meth. Appl. Mech. Eng.*, **322**, 615-632. https://doi.org/10.1016/j.cma.2017.05.007.

Shafiei, N., Mousavi, A. and Ghadiri, M. (2016c), "On size-dependent nonlinear vibration of porous and imperfect functionally graded tapered microbeams", *Int. J. Eng. Sci.*, **106**, 42-56. https://doi.org/10.1016/j.ijengsci.2016.05.007.

Shafiei, N. and She, G.-L. (2018), "On vibration of functionally graded nano-tubes in the thermal environment", *International J. Eng. Sci.*, **133**, 84-98. https://doi.org/10.1016/j.ijengsci.2018.08.004.

Shao, Y., Zhao, Y., Gao, J. and Habibi, M. (2021), "Energy absorption of the strengthened viscoelastic multi-curved composite panel under friction force", *Arch. Civil Mech. Eng.*, **21**(4), 1-29. https://doi.org/10.1007/s43452-021-00279-3.

Shariati, A., Mohammad-Sedighi, H., Żur, K.K., Habibi, M. and Safa, M. (2020), "Stability and dynamics of viscoelastic moving rayleigh beams with an asymmetrical distribution of material parameters", *Symmetry*, **12**(4), 586. https://doi.org/10.3390/sym12040586.

Sheng, C., He, G., Hu, Z., Chou, C., Shi, J., Li, J., Meng, Q., Ning, X., Wang, L. and Ning, F. (2021), "Yarn on yarn abrasion failure mechanism of ultrahigh molecular weight polyethylene fiber", *J. Eng. Fibers Fabr.*, **16**, 15589250211052766. https://doi.org/10.1177/15589250211052766.

Shivanian, E., Ghadiri, M. and Shafiei, N. (2017), "Influence of size effect on flapwise vibration behavior of rotary microbeam and its analysis through spectral meshless radial point interpolation", *Appl. Phys. A*, **123**(5), 329. https://doi.org/10.1007/s00339-017-0955-9.

Singh, A.K., Shishkin, A., Koppel, T. and Gupta, N. (2018), "A review of porous lightweight composite materials for electro-magnetic interference shielding", *Compos. Part B Eng.*, **149**, 188-197. https://doi.org/10.1016/j.compositesb.2018.05.027.

Song, Z., Liu, X., Sun, X., Li, Y., Nie, X., Tang, W., Yu, R. and Shui, J. (2019), "Alginate-templated synthesis of CoFe/carbon fiber composite and the effect of hierarchically porous structure on electromagnetic wave absorption performance", *Carbon*, **151**, 36-45. https://doi.org/10.1016/j.carbon.2019.05.025.

Su, D.H. (2014), "Application of fiber reinforced composites for sports instruments", *Appl. Mech. Mater.*, **687-691**, 4256-4259. https://doi.org/10.4028/www.scientific.net/AMM.687-691.4256.

Tang, F., Niu, B., Zong, G., Zhao, X. and Xu, N. (2022), "Periodic event-triggered adaptive tracking control design for nonlinear discrete-time systems via reinforcement learning", *Neural Networ.*, **154**, 43-55. https://doi.org/10.1016/j.neunet.2022.06.039.

Wang, H. (2013), "Application of fiber reinforced composites in sports equipment", *Appl. Mech. Mater.*, **416-417**, 1717-1720. https://doi.org/10.4028/www.scientific.net/AMM.416-417.1717.

Wang, J., Marashizadeh, P., Weng, B., Larson, P., Altan, M.C. and Liu, Y. (2022a), "Synthesis, characterization, and modeling of aligned ZnO nanowire-enhanced carbon-fiber-reinforced composites", *Materials*, **15**(7), 2618. https://doi.org/10.3390/ma15072618.

Wang, P., Gao, Z., Pan, F., Moradi, Z., Mahmoudi, T. and Khadimallah, M.A. (2022b), "A couple of GDQM and iteration techniques for the linear and nonlinear buckling of bi-directional functionally graded nanotubes based on the nonlocal strain gradient theory and high-order beam theory", *Eng. Anal. Bound. Elem.*, **143**, 124-136. https://doi.org/10.1016/j.enganabound.2022.06.007.

Wang, Z., Han, X., Wang, S., Han, X. and Pu, J. (2021), "MXene/wood-based composite materials with electromagnetic shielding properties", *Holzforschung*, **75**(5), 494-499. https://doi.org/10.1515/hf-2020-0090.

Wang, Z., Yu, S., Xiao, Z. and Habibi, M. (2020), "Frequency and buckling responses of a high-speed rotating fiber metal laminated cantilevered microdisk", *Mech. Adv. Mater. Struct.*, 1-14. https://doi.org/10.1080/15376494.2020.1824284.

Wen, S., Ren, H., Zhu, J., Bi, Y. and Zhang, L. (2019), "Fabrication of Al2O3 aerogel-SiO2 fiber composite with enhanced thermal insulation and high heat resistance", *J. Porous Mater.*, **26**(4), 1027-1034. https://doi.org/10.1007/s10934-018-0700-6.

Wu, J. and Habibi, M. (2021), "Dynamic simulation of the ultra-fast-rotating sandwich cantilever disk via finite element and semi-numerical methods", *Eng. Comput.*, 1-17. https://doi.org/10.1007/s00366-021-01396-6.

Wu, X., Gao, Y., Wang, Y., Jiang, T., Yu, J., Yang, K., Zhao, Y. and Li, W. (2020), "Preparation and mechanical properties of carbon fiber reinforced multiphase epoxy syntactic foam (CF-R-Epoxy/HGMS/CFR-HEMS Foam)", *ACS Omega*, **5**(23), 14133-14146. https://doi.org/10.1021/acsomega.0c01744.

Xie, F., Hu, W., Ning, D., Zhuo, L., Deng, J. and Lu, Z. (2018), "ZnO nanowires decoration on carbon fiber via hydrothermal synthesis for paper-based friction materials with improved friction and wear properties", *Ceram. Int.*, **44**(4), 4204-4210. https://doi.org/10.1016/j.ceramint.2017.11.224.

Xu, W., Pan, G., Moradi, Z. and Shafiei, N. (2021), "Nonlinear forced vibration analysis of functionally graded non-uniform cylindrical microbeams applying the semi-analytical solution", *Compos. Struct.*, 114395. https://doi.org/10.1016/j.compstruct.2021.114395.

Xue, B., Yang, Q., Xia, K., Li, Z., Chen, G.Y., Zhang, D. and Zhou, X. (2022), "An AuNPs/mesoporous NiO/nickel foam nanocomposite as a miniaturized electrode for heavy metal detection in groundwater", *Engineering*, in press. https://doi.org/10.1016/j.eng.2022.06.005.

Zhang, Y., Wang, Z., Tazeddinova, D., Ebrahimi, F., Habibi, M.

and Safarpour, H. (2021), "Enhancing active vibration control performances in a smart rotary sandwich thick nanostructure conveying viscous fluid flow by a PD controller", *Waves Random Complex Med*., 1-24. https://doi.org/10.1080/17455030.2021.1948627.

Zhang, H., Zhao, X., Zhang, L., Niu, B., Zong, G. and Xu, N. (2022), "Observer-based adaptive fuzzy hierarchical sliding mode control of uncertain under-actuated switched nonlinear systems with input quantization", *Int. J. Robust Nonlinear Control*, **32**(14), 8163-8185. https://doi.org/10.1002/rnc.6269.

Zhao, C., Qin, Y., Wang, X. and Xiao, H. (2022), "Coefficient of thermal expansion and mechanical properties of modified fiber-reinforced boron phenolic composites", *e-Polymers*, **22**(1), 379-388. https://doi.org/10.1515/epoly-2022-0036.

Zhao, H., Wang, H., Niu, B., Zhao, X. and Alharbi, K.H. (2023), "Event-triggered fault-tolerant control for input-constrained nonlinear systems with mismatched disturbances via adaptive dynamic programming", *Neural Netw*., **164**, 508-520. https://doi.org/10.1016/j.neunet.2023.05.001.

Zhou, C., Zhao, Y., Zhang, J., Fang, Y. and Habibi, M. (2020), "Vibrational characteristics of multi-phase nanocomposite reinforced circular/annular system", *Adv. Nano Res*., **9**(4), 295-307. https://doi.org/10.12989/anr.2020.9.4.295.

JL